

Practicality of Spin Chain Wiring in Diamond Quantum Technologies

Yuting Ping,¹ Brendon W. Lovett,^{2,1} Simon C. Benjamin,^{1,3} and Erik M. Gauger^{3,1,*}

¹*Department of Materials, University of Oxford, Oxford OX1 3PH, United Kingdom*

²*SUPA, School of Engineering and Physical Sciences, Heriot-Watt University, Edinburgh EH14 4AS, United Kingdom*

³*Centre for Quantum Technologies, National University of Singapore, 3 Science Drive 2, Singapore 117543, Republic of Singapore*
(Received 5 November 2012; published 5 March 2013)

Coupled spin chains are promising candidates for wiring up qubits in solid-state quantum computing (QC). In particular, two nitrogen-vacancy centers in diamond can be connected by a chain of implanted nitrogen impurities; when driven by suitable global fields the chain can potentially enable quantum state transfer at room temperature. However, our detailed analysis of error effects suggests that foreseeable systems may fall far short of the fidelities required for QC. Fortunately the chain can function in the more modest role as a mediator of noisy entanglement, enabling QC provided that we use subsequent purification. For instance, a chain of 5 spins with interspin distances of 10 nm has finite entangling power as long as the T_2 time of the spins exceeds 0.55 ms. Moreover we show that repurposing the chain this way can remove the restriction to nearest-neighbor interactions, so eliminating the need for complicated dynamical decoupling sequences.

DOI: [10.1103/PhysRevLett.110.100503](https://doi.org/10.1103/PhysRevLett.110.100503)

PACS numbers: 03.67.Lx, 03.65.Yz, 03.67.Hk, 75.10.Pq

Spin chains with nearest-neighbor XY coupling mediate coherent interactions between distant spin qubits with fixed locations and can thus serve as channels to transfer quantum information [1–3]. An important application would be to interconnect distant subregisters of parallel parts in a scalable, solid-state quantum computer [4], e.g., in a diamond-based architecture at room temperature [5]. With an observed room-temperature coherence time of 1.8 ms [6], the electron spin of individual nitrogen-vacancy (NV^-) defects in diamond is a promising candidate for a qubit [7]: Initialization, coherent manipulation, and measurement with nanoscale resolution (~ 150 nm) have already been experimentally demonstrated using optical techniques under ambient conditions [8]. In addition, the long-lived ^{15}N nuclear spin ($I = 1/2$) associated with each NV^- center can act as a local, coherent memory, accessible via the hyperfine coupling [9,10]. A universal set of quantum operations between the nuclear memory spin and the processing electronic spin qubit within each NV^- center is available with microwave and radio-frequency pulses [11–13]. Two NV^- centers with only a small separation ($r \lesssim 10$ nm) may be entangled through direct electron spin dipole-dipole coupling as long as a T_2 time on the order of milliseconds can be maintained [14]. However, individual addressability of the NV^- center qubits demands larger separations of several tens or hundreds of nanometers [8], and the direct interaction becomes too weak.

A recent proposal [15] suggested a chain of N implanted nitrogen impurities (each with a “dark” electronic spin-1/2) as a coherent quantum channel to transfer quantum states between distant NV^- centers at room temperature [see Fig. 1(a)]. Here, the electron spins of the NV^- centers and the nitrogen impurities interact with each other through *nearest-neighbor* dipole-dipole coupling

[16,17]. Importantly, the scheme does not require individual control of the chain spins, instead relying on global resonant driving fields to turn the effective Hamiltonian into an XY exchange model [12]. Reliable quantum state transfer (QST) between distant NV^- centers can then be achieved through this spin chain channel [15].

An important question is how well the above-described QST performs in the presence of realistic errors and imperfections [18]. In the regime $g \ll \kappa/\sqrt{N}$, the QST has been found to be surprisingly robust against disorder in the intrachain coupling κ [19,20]. The dominant error for the QST then arises due to the inevitable environmental

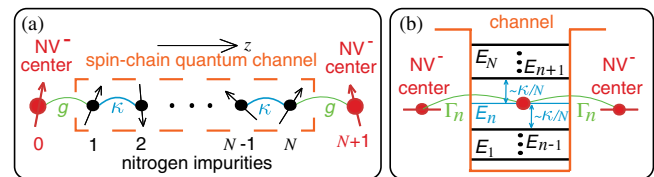


FIG. 1 (color online). (a) Two distant NV^- centers are coupled through a spin chain consisting of N nitrogen impurities; all spins are assumed to interact through nearest-neighbor dipole-dipole couplings. The intrachain and qubit-chain coupling strengths κ and g , respectively, are determined by the geometrical arrangement of the defects, and the latter can be tuned through the NV^- center ground state structure to enable high-fidelity state transfer for $g \ll \kappa/\sqrt{N}$ [15]. (b) Illustration of the equivalent fermionic tunneling picture: the channel possesses N energy levels with spacings $|E_n - E_{n\pm 1}| \sim \kappa/N$. When tuned into resonance with a channel level E_n , a NV^- spin excitation tunnels through the channel and emerges on the opposite NV^- center after a time $\tau_n = \pi/(\sqrt{2}\Gamma_n)$, where Γ_n is the effective tunneling rate. Off-resonant coupling to other levels is negligible provided that $\Gamma_n \ll |E_n - E_{n\pm 1}|$, which is equivalent to $g \ll \kappa/\sqrt{N}$ (see text).

decoherence of the spins in the channel. Focusing on such quantum noise, we argue in this Letter that this is indeed the limiting factor, and that current diamond-based architectures will fail to meet quantum error-correction thresholds while still being able to support distributed quantum information processing.

We consider the following effective Hamiltonian for a chain consisting of N spins plus two register spins located at either end of the chain (see Fig. 1):

$$H_{\text{eff}} = \sum_{i=1}^{N-1} \kappa \sigma_+^i \sigma_-^{i+1} + \sum_{j=0,N} g \sigma_+^j \sigma_-^{j+1} + \text{H.c.}, \quad (1)$$

where $\sigma_{\pm}^i = (\sigma_x^i \pm i\sigma_y^i)/2$ are the Pauli operators acting on spin i , the coupling strengths κ and g are proportional to the cubed inverse interspin distance $1/r^3$, and H.c. denotes the Hermitian conjugate. This Hamiltonian can be realized by applying global resonant microwave fields $H_{\text{drive}} = \sum_{i=0}^{N+1} \Omega_i \sigma_x^i \cos \omega_i t$ with appropriate intensities Ω_i in the presence of a constant magnetic field applied in the z direction. The ω_i denote the spin energy splittings including the Zeeman and hyperfine components [12] (see Supplemental Material [21] for more details). Importantly, the basis of the above Hamiltonian is *rotated* from the physical basis according to $(x, y, z) \rightarrow (z, -y, x)$ [12,21]. Therefore, a T_2 (T_1) process acting on the physical spin corresponds to a spin-flip (phase-flip) error in the basis adopted for the Hamiltonian equation (1).

Following Ref. [15] we proceed by applying the Jordan-Wigner transformation to Eq. (1), yielding

$$H_{\text{eff}} = \sum_{i=1}^{N-1} \kappa c_i^\dagger c_{i+1} + \sum_{j=0,N} g c_j^\dagger c_{j+1} + \text{H.c.}, \quad (2)$$

with fermion creation and annihilation operators $c_i^\dagger := \sigma_+^i \exp[-i\pi \sum_{j=0}^{i-1} \sigma_+^j \sigma_-^j]$, $c_i := \exp[i\pi \sum_{j=0}^{i-1} \sigma_+^j \sigma_-^j] \sigma_-^i$, which observe the anticommutator relations $\{c_i, c_j^\dagger\} = \delta_{ij}$ and $\{c_i, c_j\} = 0 = \{c_i^\dagger, c_j^\dagger\}$ [22]. This transforms the spin degree of freedom into the presence or absence of a fermion at the relevant system site.

For $g \ll \kappa$ the coupling of the end NV^- qubits to the channel H' can be treated perturbatively [15]. Diagonalizing the first term of Eq. (2) (and H.c.) yields

$$\tilde{H}_0 = \sum_{n=1}^N 2\kappa \cos \frac{n\pi}{N+1} f_n^\dagger f_n, \quad (3)$$

allowing us to write the second terms of Eq. (2) as follows:

$$\tilde{H}' = \sum_{n=1}^N \Gamma_n [c_0^\dagger f_n + (-1)^{n-1} c_{N+1}^\dagger f_n + \text{H.c.}], \quad (4)$$

where $f_n^\dagger = \sum_{j=1}^N \sin \frac{jn\pi}{N+1} c_j^\dagger / \sqrt{(N+1)/2}$ and $\Gamma_n = g \sin \frac{n\pi}{N+1} / \sqrt{(N+1)/2}$ for $n = 1, 2, \dots, N$ [22–24]. The channel is now described by \tilde{H}_0 and possesses N modes with energies

$E_n = 2\kappa \cos \frac{n\pi}{N+1}$. One can tune the energy of both NV^- centers to E_n by means of applying an appropriate detuning to $S_z^{0,N+1}$ in the rotated basis. This couples the NV^- centers resonantly to the channel mode n with a tunneling rate Γ_n [see Fig. 1(b)]. Based on pure Hamiltonian evolution, the first full swap of the two end fermions occurs after a time

$$t_n = \frac{\pi}{\sqrt{2}\Gamma_n} = \frac{\pi\sqrt{N+1}}{2g \sin \frac{n\pi}{N+1}}. \quad (5)$$

The final swapped state acquires a controlled phase depending on the total number of fermions in the system [15,25]. Because for $g \ll \kappa/\sqrt{N}$ off-resonant coupling to other channel modes is negligible, the phase arises from the single mode and, while generally unknown at finite temperature, is well defined; it can then be corrected by employing a two-round protocol [12,15,21,26]. Based on this protocol, single-mode coupling QST is *independent* of the initial chain state.

It is readily seen that the tunneling rate Γ_n reaches its maximal value for odd N and $n = (N+1)/2$ with $E_n = 0$. In this case, no detuning is required, and the end NV^- qubits resonantly couple to the zero-energy mode of the channel. We adopt this case of odd N as the ideal implementation of the protocol. Because our calculations are not restricted to the single excitation subspace used in Ref. [19], we specifically consider the two cases of $N = 3$ and $N = 5$ resulting in simulations involving six and eight spins (chain plus two registers and one ancilla) as explained further on. We simulate the full system dynamics by numerically integrating a Lindblad master equation [21,27] using Hamiltonian equation (1). Unless stated otherwise, we take the interspin spacing in the chain to be $r_{N,N} = 10$ nm ($\kappa = 26$ kHz) while g remains fully tuneable.

Numerous studies seek to determine a threshold below which scalable quantum computing is in principle possible. Typically, papers quote the threshold obtained by equating the error rates in state preparation, measurement, and qubit-qubit operations (generally, the latter are the most crucial). For qubits embedded in diamond and linked by spin chains, the most relevant thresholds are those for architectures where qubits are arranged on a latticelike structure with each qubit being wired to only a few others. For this case, the threshold error rate is on the order of 1%, e.g., 0.75% for the widely studied topologically protected cluster-state approach [28], while 1.4% can be obtained in *certain* circumstances [29]. Here we will take a target error rate of 1%, i.e., a fidelity requirement of 99%. Note that to avoid diverging resource requirements, one would not wish to build a computer with performance *near* the threshold; practically one might target an error rate ten times below the threshold [30]. We demonstrate in the Supplemental Material [21] that the threshold 1% rate requires a physical T_2 time of 16 ms for the $N = 5$ chain when using an optimally tuned ratio of g/κ [31]. By contrast, the longest measured T_2 time of the NV^- center is an order of magnitude below this number at 1.8 ms [6]. Reported coherence

times of the nitrogen impurity are much shorter (e.g., $5.5 \mu\text{s}$ at room temperature and $80 \mu\text{s}$ at 2.5 K [32]). While this should be improvable, the nitrogen impurity is unlikely to substantially surpass the NV^- center [21]. In reality, chains longer than $N = 5$ will be desirable to properly separate the NV^- centers. We therefore conclude that using QST as a fault-tolerant two-qubit operation may well be an infeasible target for any foreseeable technology.

Nonetheless, the suggested spin chain quantum bus may still be able to support the distribution of entanglement, opening the possibility of employing distillation protocols to create high-fidelity entanglement over several runs [33]. Recent studies show that highly imperfect intersite links can be tolerated given that one has three or four qubits at each local site [34,35]. The key enabling property of the channel is then simply that it should be “quantum” in contrast to “classical,” i.e., a channel that is capable of transmitting a finite amount of entanglement with each run. Identifying the transition from quantum to classical channel with respect to realistic decoherence processes is the main purpose of this Letter. To address this question we attempt to transfer one half of a Bell state through the channel. More specifically, the near ($i = 0$) NV^- center starts off in a maximally entangled singlet state with an additional ancilla spin, $|\Psi^-\rangle = (|0\rangle_a|1\rangle_0 - |1\rangle_a|0\rangle_0)/\sqrt{2}$, and our observable is the entanglement of formation E_F [36] between this ancilla and the remote NV^- center at position $N + 1$ [37].

Let us start with $N = 3$ as the shortest nontrivial odd chain [38]. Figure 2(a) shows that this channel is robust against physical spin-flip (i.e., T_1 type [39]) errors, which act as phase-flip errors in the basis of Eq. (1). A high degree of transferred entanglement is achievable for $T_1 > 1 \text{ ms}$, and a finite amount of entanglement survives in the presence of much larger error rates. Longer chains also remain robust against this type of error; for the single excitation subspace, we have simulated odd chains up to $N = 21$ obtaining similar qualitative results [21]. Further, we have confirmed that this behavior is independent of the initial chain state, and that our results are in agreement with Ref. [19].

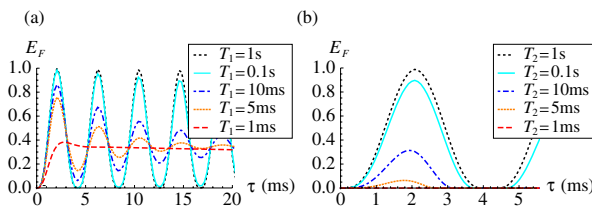


FIG. 2 (color online). Entanglement of formation E_F between the ancilla and the remote NV^- center qubit as a function of the transfer time τ under an independent (a) spin-flip and (b) phase-flip error model for the nitrogen spins ($N = 3$). The errors are applied as Lindblad operators on each chain spin: (a) $L_i = \sigma_{z_i}$ with rate $\gamma = 1/T_1$; (b) $L_i = \sigma_{x_i}$ with rate $\gamma = 1/T_2$. The initial state is $|\Psi^-\rangle_{a0}|000\rangle_{N+1}$, and $g = \kappa/(10\sqrt{N})$.

On the other hand, dephasing of the physical spins, characterized by their T_2 time, induces spin-flip errors in the computational basis, with a much more damaging effect on the entangling power of the channel [see Fig. 2(b)]. For weak coupling between the NV^- centers and the channel, the QST becomes classical; i.e., E_F vanishes completely, for $T_2 \leq 3.2 \text{ ms}$. Applying the same model to the $N = 5$ chain, the transition between a classical and a quantum channel occurs at $T_2 = 7.6 \text{ ms}$. This threshold increases further for larger N due to the transfer time becoming longer [see Eq. (5)], as effectively more spins are exposed to the noise for longer.

Unlike the high-fidelity transfer of a particular quantum state, entanglement distribution does not benefit from coupling to only a single channel mode, allowing us to explore stronger coupling by varying g . Figure 3(a) shows the T_2 threshold that separates the quantum from the classical data bus for chains with $N = 3$ and $N = 5$, and we see that the highest tolerable dephasing rate occurs in the interval $g \in (0.8\kappa, \kappa)$. Expressed as a T_2 time threshold this gives 0.25 ms (0.55 ms) for the $N = 3$ ($N = 5$) chain with $r_{N,N} = 10 \text{ nm}$.

In Figs. 3(b) and 3(c), we show the entangling capacity of the $N = 3$ and $N = 5$ channels as a function of g and the dephasing rate $\gamma = 1/T_2$. We note that high channel entangling power is only realized for a small decoherence rate of

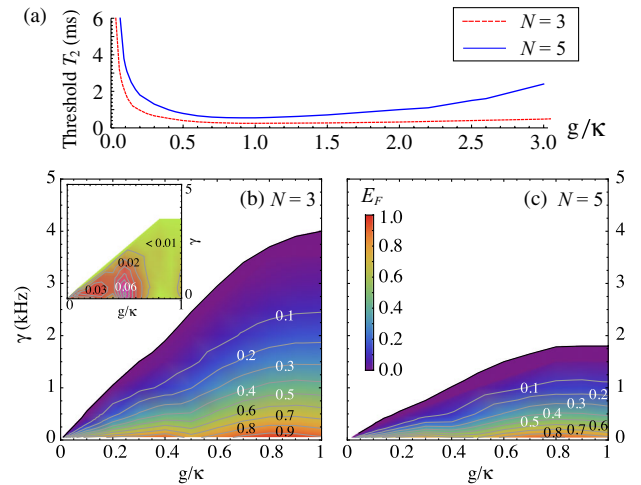


FIG. 3 (color online). (a) T_2 threshold separating classical ($E_F = 0$) and quantum ($E_F > 0$) state transfer. The initial chain states are $|\Psi^-\rangle_{a0}|000\rangle_{N+1}$ and $|\Psi^-\rangle_{a0}|00000\rangle_{N+1}$, respectively, but the threshold for other initial states is similar. (b) and (c) Maximally achievable entanglement of formation E_F between the ancilla spin and the remote NV^- center spin as a function of g/κ and independent channel spin-flip rate $\gamma = 1/T_2$ for $N = 3$ and $N = 5$. The channel is entirely classical in the white regions. The inset in (b) shows the variation in E_F occurring for the eight different computational basis states of the channel spins in the $N = 3$ case; in all cases the range of values of E_F is small and always less than 0.07 . Random checks for the $N = 5$ case suggest a similar behavior for longer chains.

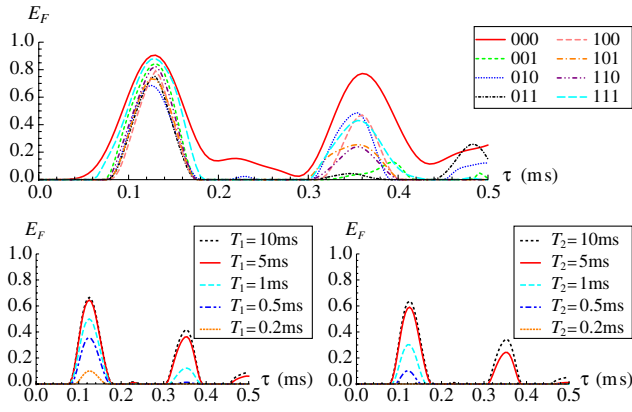


FIG. 4 (color online). Top: E_F between the ancilla spin and the remote NV^- center as a function of the transfer time τ for all eight initial chain states of the $N = 3$ non-nearest-neighbor chain. All spins are assumed equally spaced, with the coupling strength for nearest neighbors being 26 kHz. Bottom: E_F for the initial state $|\Psi^-\rangle_{a0}|010\rangle|0\rangle_{N+1}$ with decoherence processes of independent phase-flip noise (left) and spin-flip noise (right) in the basis of Hamiltonian equation (1) corresponding to physical T_1 and T_2 processes, respectively.

the nitrogen spins, even for larger g . Unsurprisingly, the channel is highly inefficient close to the classical threshold.

To connect two NV^- centers separated by a fixed distance of 40 nm, we consider a chain comprising three and five nitrogen spins. In both cases the register spins are assumed to be 10 nm away from the ends of the chain, so that the chain's interspin distances are $r_{N,N} = 10$ nm and $r_{N,N} = 5$ nm, respectively. The first case then corresponds to the $N = 3$ chain we have studied so far, but for the $N = 5$ case we obtain a minimal $T_2 \approx 70 \mu\text{s}$ for quantum communication (for $g = \kappa$), which is significantly shorter than 0.25 ms for the $N = 3$ chain. The benefit of stronger coupling therefore outweighs the drawback of a longer chain for a fixed separation between the register spins by speeding up the transfer process. However, how many impurity spins can be deployed will crucially depend on the achievable implantation precision, since even subnanometer imperfections entail significant coupling disorder for closely spaced chains.

So far, we have assumed nearest-neighbor couplings [see Eq. (1)], which could be realized through dynamical decoupling [12]. In practice, one needs a coupling strength “high pass filter,” which would typically reduce effective coupling strengths and add further complexity to experimental implementations. We now relax this assumption and include all pairwise couplings with a dipole-dipole interaction $1/r^3$ distance dependence (similar to Refs. [40,41]), including register to chain spin couplings.

Figure 4 demonstrates that the entanglement transfer for a uniformly spaced spin chain now depends on the initial chain state. However, the first maximum of all initial states coincides and gives rise to a reasonable degree of transferred entanglement. Thus we pick the initial chain state

$|\Psi^-\rangle_{a0}|010\rangle|0\rangle_{N+1}$ as an example that is indicative of the performance to be expected. Interestingly, T_1 and T_2 type processes degrade the E_F with much more similar severity compared to the nearest-neighbor-only coupling case [42]. Nonetheless, there still exists a threshold in the T_2 coherence time, and to ensure quantum communication for an arbitrary initial state, we require $T_2 > 0.28$ ms, which is only slightly longer than for the nearest-neighbor chain. For the case of the $N = 5$ chain (not shown), we have determined the transition threshold to be $T_2 > 0.67$ ms, which again only represents a modest increase. Taking into account the complexity and expected reduction in effective coupling strengths from dynamical decoupling sequences, it may thus be more practical to drop the restriction of only nearest-neighbor interactions. As we show in the Supplemental Material [21], the state transfer still remains similarly robust to small coupling-strength disorder [21].

In conclusion, by employing numerical simulations we have studied the impact of inevitable decoherence processes on the entanglement capacity of a spin chain bus that is realized by dipole-dipole coupling of crystal defects. Limiting our discussion to chains of length $N = 3$ and $N = 5$ as likely candidates for a first experimental demonstration (and also for numerical tractability) has allowed us to obtain insight into important characteristics of such a protocol in the presence of realistic noise. Our conclusions will be equally relevant for longer chains, which are known to be even more susceptible to decoherence [43–45]. We have shown that directly meeting quantum error-correction thresholds remains infeasible even if all spins possessed the exceptional coherence time of NV^- centers. In contrast, the distribution of a finite amount of entanglement appears realistic with current systems, offering the possibility of applying distillation protocols to boost the transmitted entanglement with additional local operations and classical communication [33].

The authors are grateful to Earl Campbell and Jason Smith for useful discussions. This work was supported by the National Research Foundation, the Ministry of Education, Singapore. B.W.L. acknowledges the Royal Society for a University Research Fellowship. Y.P. thanks Hertford College, Oxford, for support from their scholarship program.

*erik.gauger@nus.edu.sg

- [1] S. Bose, *Phys. Rev. Lett.* **91**, 207901 (2003).
- [2] M. Christandl, N. Datta, A. Ekert, and A. J. Landahl, *Phys. Rev. Lett.* **92**, 187902 (2004).
- [3] M.-H. Yung and S. Bose, *Phys. Rev. A* **71**, 032310 (2005).
- [4] S. Lloyd, *Science* **261**, 1569 (1993).
- [5] A. M. Stoneham, A. H. Harker, and G. W. Morley, *J. Phys. Condens. Matter* **21**, 364222 (2009).
- [6] G. Balasubramanian *et al.*, *Nat. Mater.* **8**, 383 (2009).
- [7] F. Jelezko, T. Gaebel, I. Popa, A. Gruber, and J. Wrachtrup, *Phys. Rev. Lett.* **92**, 076401 (2004).

- [8] P. C. Maurer *et al.*, *Nat. Phys.* **6**, 912 (2010).
- [9] G. D. Fuchs, G. Burkard, P. V. Klimov, and D. D. Awschalom, *Nat. Phys.* **7**, 789 (2011).
- [10] M. V. G. Dutt, L. Childress, L. Jiang, E. Togan, J. Maze, F. Jelezko, A. S. Zibrov, P. R. Hemmer, and M. D. Lukin, *Science* **316**, 1312 (2007).
- [11] P. Cappellaro, L. Jiang, J. S. Hodges, and M. D. Lukin, *Phys. Rev. Lett.* **102**, 210502 (2009).
- [12] N. Y. Yao, L. Jiang, A. V. Gorshkov, P. C. Maurer, G. Giedke, J. I. Cirac, and M. D. Lukin, *Nat. Commun.* **3**, 800 (2012).
- [13] L. Childress, M. V. G. Dutt, J. M. Taylor, A. S. Zibrov, F. Jelezko, J. Wrachtrup, P. R. Hemmer, and M. D. Lukin, *Science* **314**, 281 (2006).
- [14] P. Neumann *et al.*, *Nat. Phys.* **6**, 249 (2010).
- [15] N. Y. Yao, L. Jiang, A. V. Gorshkov, Z.-X. Gong, A. Zhai, L.-M. Duan, and M. D. Lukin, *Phys. Rev. Lett.* **106**, 040505 (2011).
- [16] R. J. Epstein, F. M. Mendoza, Y. K. Kato, and D. D. Awschalom, *Nat. Phys.* **1**, 94 (2005).
- [17] R. Hanson, F. M. Mendoza, R. J. Epstein, and D. D. Awschalom, *Phys. Rev. Lett.* **97**, 087601 (2006).
- [18] A. Zwick, G. A. Álvarez, J. Stolze, and O. Osenda, *Phys. Rev. A* **84**, 022311 (2011).
- [19] N. Y. Yao *et al.*, [arXiv:1206.0014](https://arxiv.org/abs/1206.0014).
- [20] A. Zwick, G. A. Alvarez, J. Stolze, and O. Osenda, *Phys. Rev. A* **85**, 012318 (2012).
- [21] See Supplemental Material at <http://link.aps.org/supplemental/10.1103/PhysRevLett.110.100503> for more information about our model and additional calculations.
- [22] E. Lieb, T. Schultz, and D. Mattis, *Ann. Phys. (N.Y.)* **16**, 407 (1961).
- [23] A. Wójcik, T. Łuczak, P. Kurzyński, A. Grudka, T. Gdala, and M. Bednarska, *Phys. Rev. A* **72**, 034303 (2005).
- [24] L. C. Venuti, S. M. Giampaolo, F. Illuminati, and P. Zanardi, *Phys. Rev. A* **76**, 052328 (2007).
- [25] S. R. Clark, C. M. Alves, and D. Jaksch, *New J. Phys.* **7**, 124 (2005).
- [26] M. Markiewicz and M. Wieśniak, *Phys. Rev. A* **79**, 054304 (2009).
- [27] H.-P. Breuer and F. Petruccione, *The Theory of Open Quantum Systems* (Oxford University Press, New York, 2002).
- [28] R. Raussendorf and J. Harrington, *Phys. Rev. Lett.* **98**, 190504 (2007); R. Raussendorf, J. Harrington, and K. Goyal, *New J. Phys.* **9**, 199 (2007).
- [29] D. S. Wang, A. G. Fowler, and L. C. L. Hollenberg, *Phys. Rev. A* **83**, 020302(R) (2011).
- [30] A. G. Fowler, M. Mariantoni, J. M. Martinis, and A. N. Cleland, *Phys. Rev. A* **86**, 032324 (2012).
- [31] Interestingly, the required T_1 time, causing phase flips in the computational basis, may be much shorter; see Ref. [19].
- [32] S. Takahashi, R. Hanson, J. van Tol, M. S. Sherwin, and D. D. Awschalom, *Phys. Rev. Lett.* **101**, 047601 (2008).
- [33] C. H. Bennett, H. J. Bernstein, S. Popescu, and B. Schumacher, *Phys. Rev. A* **53**, 2046 (1996); C. H. Bennett, G. Brassard, S. Popescu, B. Schumacher, J. A. Smolin, and W. K. Wootters, *Phys. Rev. Lett.* **76**, 722 (1996); C. H. Bennett, D. P. DiVincenzo, J. A. Smolin, and W. K. Wootters, *Phys. Rev. A* **54**, 3824 (1996).
- [34] Y. Li and S. C. Benjamin, *New J. Phys.* **14**, 093008 (2012).
- [35] K. Fujii, T. Yamamoto, M. Koashi, and N. Imoto, [arXiv:1202.6588](https://arxiv.org/abs/1202.6588).
- [36] W. K. Wootters, *Phys. Rev. Lett.* **80**, 2245 (1998).
- [37] The phase acquired during the swap maps the singlet to a Bell equivalent state without degrading the quality of entanglement.
- [38] All channels with $N > 1$ possess more than one mode [2], so perfect QST for all values of g is limited to $N = 1$.
- [39] We here take the inverse spin-flip error rate as the T_1 time; this is not strictly the same as a T_1 time from energy relaxation.
- [40] A. Kay, *Phys. Rev. A* **73**, 032306 (2006).
- [41] R. Ronke, T. Spiller, and I. D'Amico, *J. Phys. Conf. Ser.* **286**, 012020 (2011).
- [42] Restoring nearest-neighbor coupling only for the register spins largely reintroduces the asymmetric behavior with respect to the two different types of noise.
- [43] J.-M. Cai, Z.-W. Zhou, and G.-C. Guo, *Phys. Rev. A* **74**, 022328 (2006).
- [44] M. L. Hu and H. L. Lian, *Eur. Phys. J. D* **55**, 711 (2009); M. L. Hu, *Eur. Phys. J. D* **59**, 497 (2010).
- [45] T.-H. Zeng, B. Shao, and J. Zou, *Chin. Phys. Lett.* **26**, 020313 (2009).